








Design and synthesis of bioreductive prodrugs of class I histone deacetylase inhibitors and their biological evaluation in virally transfected acute myeloid leukemia cells

Mohamed Abdelsalam^{1,2}  | Mariia Zmyslia³ | Karin Schmidtkunz⁴ | Anita Vecchio¹ | Sebastian Hilscher⁵  | Hany S. Ibrahim^{1,6}  | Mike Schutkowski⁵  | Manfred Jung^{4,7}  | Claudia Jessen-Trefzer³  | Wolfgang Sippl¹ 

¹Department of Medicinal Chemistry, Martin-Luther University of Halle-Wittenberg, Halle/Saale, Germany

²Department of Pharmaceutical Chemistry, Faculty of Pharmacy, Alexandria University, Alexandria, Egypt

³Institute of Organic Chemistry, University of Freiburg, Freiburg i. Br., Germany

⁴Institute of Pharmaceutical Sciences, University of Freiburg, Freiburg i. Br., Germany

⁵Department of Enzymology, Institute of Biochemistry, Martin-Luther-University of Halle-Wittenberg, Halle/Saale, Germany

⁶Department of Pharmaceutical Chemistry, Faculty of Pharmacy, Egyptian Russian University, Cairo, Egypt

⁷CIBSS – Centre for Integrative Biological Signalling Studies, University of Freiburg, Freiburg i. Br., Germany

Correspondence

Claudia Jessen-Trefzer, Institute of Organic Chemistry, University of Freiburg, Freiburg i. Br. 79104, Germany.
Email: claudia.jessen-trefzer@pharmazie.uni-freiburg.de

Wolfgang Sippl, Department of Medicinal Chemistry, Institute of Pharmacy, Martin-Luther University of Halle-Wittenberg, Halle/Saale 06120, Germany.
Email: wolfgang.sippl@pharmazie.uni-halle.de

Funding information

Excellence Strategy of the German Federal and State Governments, Grant/Award Number: CIBSS–EXC 2189; Deutsche Forschungsgemeinschaft (DFG), Grant/Award Numbers: 278002225/RTG 2202, 469954457, 471614207; Alexander von Humboldt Foundation Project, Grant/Award Number: EGY 1191187

Abstract

Although histone deacetylase (HDAC) inhibitors show promise in treating various types of hematologic malignancies, they have some limitations, including poor pharmacokinetics and off-target side effects. Prodrug design has shown promise as an approach to improve pharmacokinetic properties and to improve target tissue specificity. In this work, several bioreductive prodrugs for class I HDACs were designed based on known selective HDAC inhibitors. The zinc-binding group of the HDAC inhibitors was masked with various nitroarylmethyl residues to make them substrates of nitroreductase (NTR). The developed prodrugs showed weak HDAC inhibitory activity compared to their parent inhibitors. The prodrugs were tested against wild-type and NTR-transfected THP1 cells. Cellular assays showed that both 2-nitroimidazole-based prodrugs **5** and **6** were best activated by the NTR and exhibited potent activity against NTR-THP1 cells. Compound **6** showed the highest cellular activity ($GI_{50} = 77$ nM) and exhibited moderate selectivity. Moreover, activation of prodrug **6** by NTR was confirmed by liquid chromatography-mass spectrometry analysis, which showed the release of the parent inhibitor after incubation with *Escherichia coli* NTR. Thus, compound **6** can be considered a novel prodrug selective for class I HDACs, which could be used as a good starting point for increasing selectivity and for further optimization.

This is an open access article under the terms of the [Creative Commons Attribution-NonCommercial-NoDerivs](https://creativecommons.org/licenses/by-nc-nd/4.0/) License, which permits use and distribution in any medium, provided the original work is properly cited, the use is non-commercial and no modifications or adaptations are made.

© 2023 The Authors. *Archiv der Pharmazie* published by Wiley-VCH GmbH on behalf of Deutsche Pharmazeutische Gesellschaft.

KEYWORDS

epigenetics, HDACs, hypoxia, nitroreductases, prodrugs

1 | INTRODUCTION

Reversible histone acetylation is a key posttranslational modification that regulates gene expression by modifying chromatin architecture.^[1,2] This process is controlled by two opposing enzyme families. Histone acetyltransferases (HATs) catalyze the addition of an acetyl or acyl group on the ϵ -amino group of lysine residues of histone proteins.^[3] These modifications result in neutralizing the positive charge on lysine residues, reducing the interactions between histone proteins and DNA, and finally leading to gene-transcription activation.^[2,3] The histone deacetylases (HDACs) remove the acetyl or acyl groups from the modified lysine residues, resulting in the formation of condensed chromatin and transcriptional gene silencing.^[2,4] In humans, 18 different HDACs have been identified and classified according to their sequence homology to yeast into four classes. Class I (HDAC1–3, and 8), class II (HDAC4–7, 9, and 10), and class IV (HDAC11), which are zinc-dependent deacetylases, and class III (sirtuins SIRT1–7), which are NAD⁺-dependent deacetylases.^[4,5] Besides acting on modified lysine residues of histones, HDACs have numerous nonhistone substrates.^[2,5,6] Recently, HDACs have gained growing interest as potential therapeutic targets as these enzymes can modify the aberrant epigenetic conditions associated with cancer development.^[6,7] Several HDAC inhibitors (HDACi) have been developed and tested as potential therapies for solid tumors and blood malignancies.^[8–10] Most HDACi share a common pharmacophoric feature consisting of three distinct groups as follows: a zinc-binding group (ZBG), a capping group, and a linker.^[11] The ZBG is responsible for chelating Zn²⁺ ion in the active site of HDACs. Different ZBGs have been used for the development of HDACi, for example, hydroxamic acids, 2-aminobenzamides, short-chain fatty acids, thiols, alkylhydrazides, and others.^[12,13] In addition, cyclic peptides without a ZBG have been reported as HDACi.^[14] To date, four HDACi have been approved by the US Food and Drug Administration (FDA) for the treatment of different types of hematological malignancies. These include the hydroxamate-based inhibitors vorinostat, belinostat, and panobinostat, as well as the thiol-prodrug/depsipeptide (romidepsin).^[11] Although hydroxamic acid is a potent and widely used ZBG, it was observed that hydroxamate-based HDAC inhibitors often lack HDAC-isoform selectivity and show off-target side effects.^[15,16] In addition, they are associated with cellular mutagenicity and genotoxicity.^[17] Compared with hydroxamate-based HDACi, the 2-aminobenzamide HDACi exhibit improved class I HDAC selectivity and lower toxicity (Figure 1).^[18,19] Several clinical studies revealed that hematological toxicities associated with HDACi may limit their therapeutic window, and this is a main reason to exclude several potent candidates from further drug development.^[20–22] Therefore, cell-specific inhibition of such epigenetic targets could be a promising strategy to overcome off-target side effects.

One of the approaches that can be applied to enhance targeted-tissue specificity and to improve drug delivery to selected cell types is the design of prodrugs.^[23] Prodrugs are themselves inactive, but through chemical or enzymatic cleavage, the bioactive form of drugs can be released. Also, by exploiting tumor-intrinsic factors, a cancer-specific release might be obtained.^[23,24] One of these factors is hypoxia, which is a deficiency in oxygen supply reaching the tissues and contributes to the chemotherapeutic resistance of tumors.^[25] Hypoxia induces high expression of reductase enzymes; therefore, hypoxia has evolved as a promising approach in the design of anticancer agents.^[26,27] Additionally, several hypoxia-activated chemotherapeutic agents are currently in clinical development.^[26] The directed enzyme prodrug therapy (DEPT) principle is one of the strategies that can be applied for selective targeting of exogenous enzymes to cancer cells. This approach allows site-specific release of the active drug by an exogenous enzyme that is either linked to an antibody (ADEPT) or encoded by a gene that is targeted to the tumor site (GDEPT).^[28] Nitroreductase (NTR) is one of the enzymes that can be used for the DEPT approach.^[28] NTR is a bacterial oxygen-insensitive homodimeric flavoenzyme encoded by the *nfsB* gene.^[29,30] The NTR catalyzes the reduction of the nitro group of various nitroaromatic substrates such as 4-nitrobenzyl and 1-methyl-2-nitroimidazolyl carbamates of cytotoxic amines to the corresponding nitroso intermediate, which is further reduced to the hydroxylamine derivative, followed by self-immolation and fragmentation to release the active inhibitor, in addition to a Michael acceptor and CO₂ as side products (Figure 2).^[31–33]

There is ample evidence for the presence of reducing enzymes in hypoxic tumors, including but not limited to enzymes able to reduce nitroaromatic compounds.^[27] For example, a NTR enzyme has been isolated from Walker 256 rat carcinoma cells, which can convert CB 1954 to a cytotoxic DNA interstrand crosslinking agent by reduction of its 4-nitro group to the corresponding hydroxylamino species.^[34] Interestingly, inhibition of drug reduction by oxygen through redox cycling mechanism was first demonstrated for nitro compounds and was subsequently shown to be responsible for the hypoxia-selective cytotoxicity of nitroimidazole. In the current study, we have worked with a bacterial enzyme (NTR from *Escherichia coli*), since it is well-known mimic of hypoxic conditions.

1-Methyl-2-nitroimidazole has been identified as a good masking group for NTR substrates, which is characterized by fast unmasking, and it has been further used as a prodrug moiety for the cell-specific delivery of several chemotherapeutic agents.^[25,35] Recently, the NTR-activated prodrug approach has been successfully applied for the design of different epigenetic inhibitors, such as the hydroxamate-based HDACi vorinostat (SAHA)^[36] and the lysine-specific histone demethylase 1 (LSD1) tranylcypromine.^[37] In the present study, we used this system to develop a research tool to study the effects of selective HDAC1–3 inhibitors in targeted cells which, as noncytotoxic agents, also allow the study of the effect of the Michael acceptor that is formed upon enzymatic uncaging. We

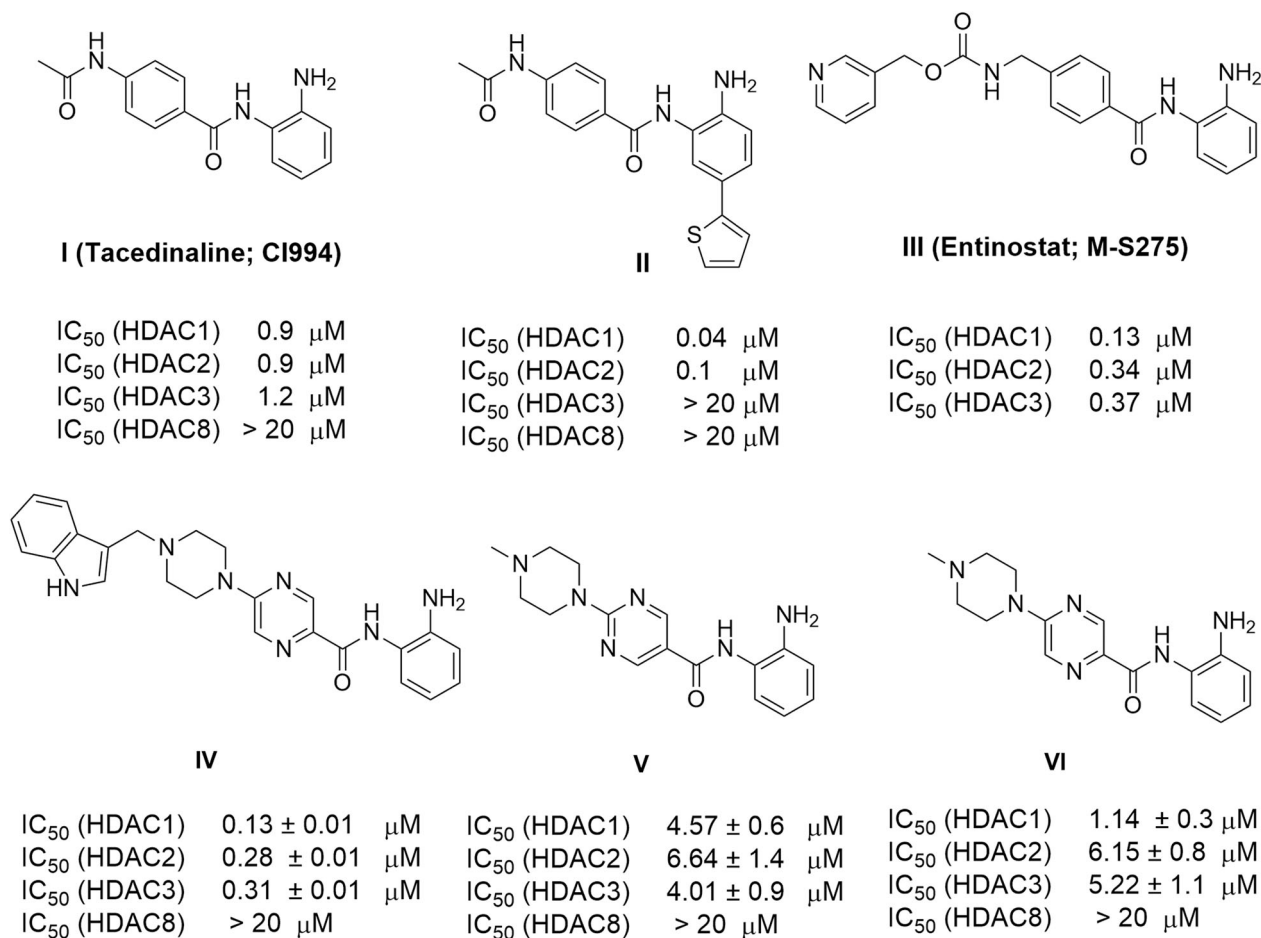


FIGURE 1 Examples of 2-aminobenzamide-histone deacetylase (HDAC) inhibitors and their inhibitory activity toward different HDAC isoforms.^[18,19]

developed different nitroaryl-based NTR prodrugs for HDAC1–3 using previously developed aminobenzamide-based HDAC inhibitors. Furthermore, the biological activity of the newly synthesized prodrugs is evaluated against acute myeloid leukemia (AML) cells using an NTR enzyme-prodrug system.

2 | RESULTS AND DISCUSSION

2.1 | Chemistry

For the design of the prodrugs, different reported HDAC1–3 inhibitors (I–II and IV–VI; Figure 1) were selected, and their aminobenzamide group was masked with different nitroaryl alcohols, such as 4-nitrobenzyl or 1-methyl-2-nitroimidazolyl alcohols (Figure 2), through a carbamate linker. This attachment should result in reducing the binding to the targeted protein (since such sterically demanding groups are not accepted by the narrow HDAC1–3 binding tunnel), and accordingly, the HDAC inhibitory activity of these prodrugs is expected to decrease. In addition, the carbamate linker was chosen as it is *in vivo* more stable compared to corresponding carbonates or ester groups.^[38] Additionally, the carbamic acid

formed after the elimination of the nitroaromatic prodrug moiety can undergo fast and irreversible self-immolation, which finally results in the formation of the free aminobenzamide and CO₂, as shown in Figure 2.^[39]

To obtain the 2-nitroimidazole-based prodrugs, we planned a three-step synthetic scheme. The first step involved the synthesis of different reported 2-aminobenzamides I–II and IV–VI, which were synthesized according to previously reported procedures.^[18,19,40] The second step was the synthesis of 1-methyl-2-nitro-1H-imidazole-5-methanol (1), which was prepared according to our previously reported method.^[37] Then, the alcohol intermediate 1 was activated using 4-nitrophenyl chloroformate (2) in the presence of pyridine to obtain the corresponding 4-nitrophenyl carbonate derivative 3. Finally, condensation of the activated nitroimidazole intermediate 3 with the appropriate 2-aminobenzamides I–II and IV–VI in the presence of hydroxybenzotriazole (HOBt) afforded the corresponding prodrugs 4–8 (Scheme 1). Regarding the synthesis of the 4-nitrobenzyl-based prodrugs 10–12, the commercially available 4-nitrobenzyl chloroformate (9) was reacted with the appropriate amine in the presence of potassium carbonate to get the corresponding prodrug 10–12 as shown in Scheme 2.

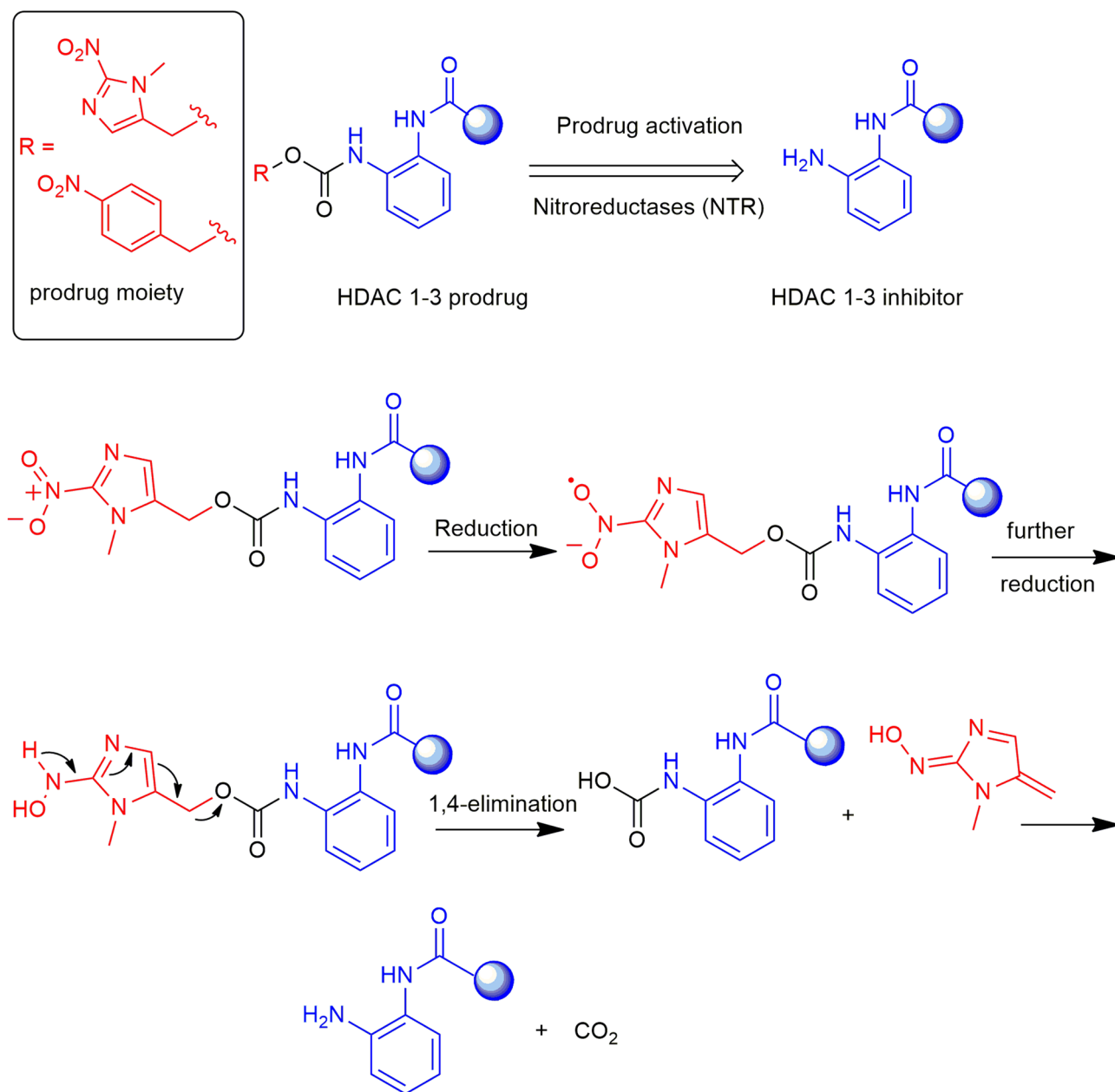


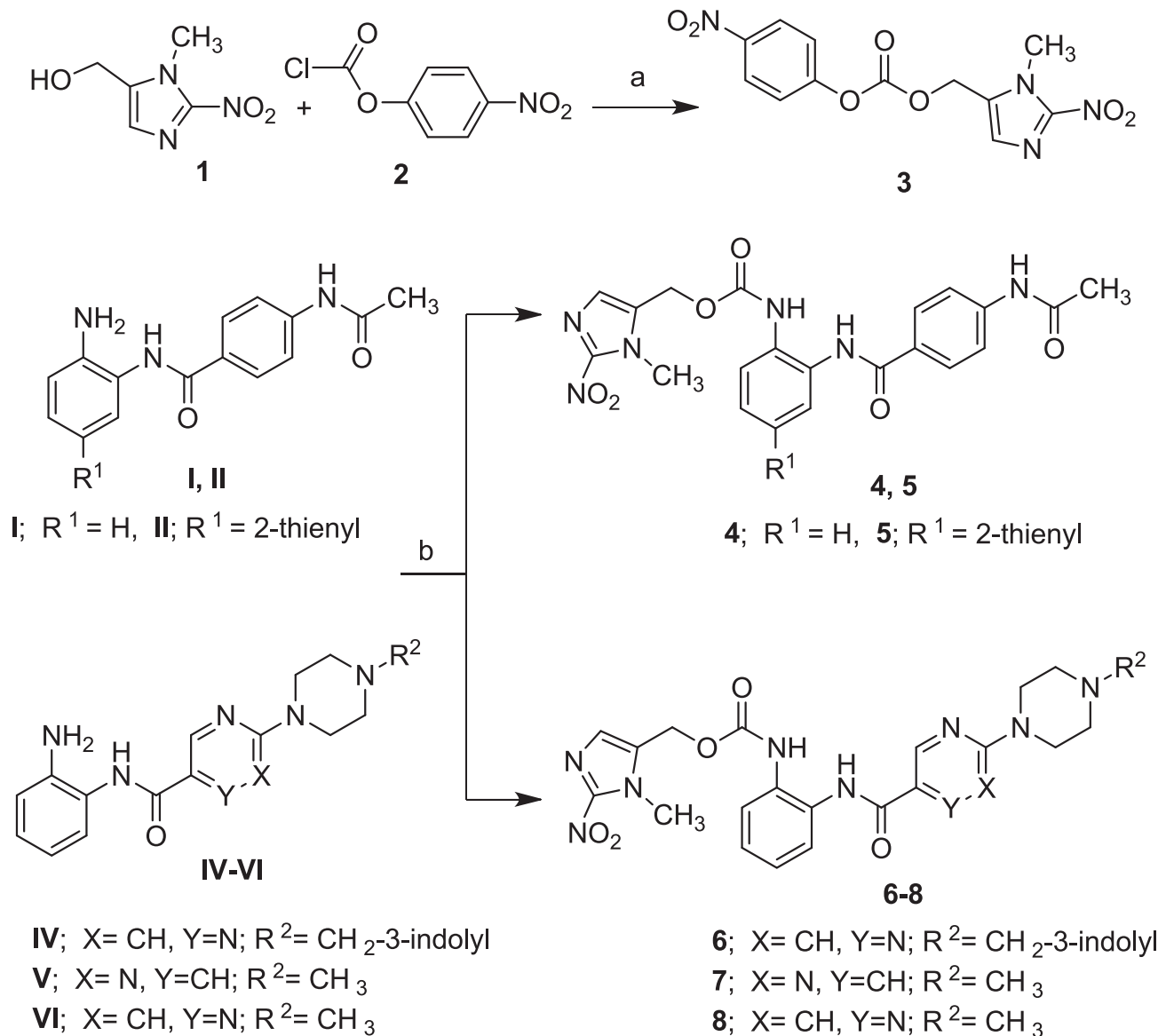
FIGURE 2 The rationale for the design of novel histone deacetylase (HDAC)1–3 prodrugs based on different 2-aminobenzamides and the postulated schematic pathway of HDAC inhibitor release.

2.2 | Biology

2.2.1 | In vitro testing of HDAC inhibitory activity

The synthesized prodrugs, in addition to the parent HDAC inhibitors, were tested for their inhibitory activity against human class I HDACs (HDAC1–3) using a fluorogenic peptide derived from p53 (Ac-RHKK (Acetyl)-AMC) (Table 1).^[41] The prodrugs were tested against HDAC1–3 at three different concentrations (10, 1, and 0.1 μM) (Supporting Information S1: Table 1). As previously described,^[18,42] compounds IV–VI were designed as a novel series of class I HDAC inhibitors based on different structural modifications of the general

scaffold of the reported HDAC1–3 inhibitors tacedinaline (I) and entinostat (III). For the previously developed HDAC inhibitors,^[18,42] we showed target engagement by measuring the hyperacetylation on H3K9 (HDAC1 substrate). For the developed inhibitors, the phenyl ring in the middle of tacedinaline was replaced with the more polar pyrazine ring as in the case of compound VI, which showed improved inhibitory activity against HDAC1–3 compared to tacedinaline (Table 1). On the other hand, the replacement of the phenyl ring with a pyrimidine ring, as in the case of compound V, resulted only in a slight decrease in the inhibitory activity against HDAC1 compared to compound VI. The second modification involved the replacement of the middle phenyl ring of entinostat with a pyrazine ring, in



SCHEME 1 Synthesis of 1-methyl-2-nitro-1H-imidazolyl-based prodrugs 4–8. Reagents and conditions: (a) pyridine, tetrahydrofuran (THF), RT, overnight, 33.8%; (b) intermediate (3), hydroxybenzotriazole (HOBT), *N,N*-dimethylformamide (DMF), RT, overnight, 23%–64%.

addition to the replacement of the pyridine ring (capping group) with the bulkier 3-indolyl scaffold as in the case of compound **IV**, which resulted in higher inhibitory activity against HDAC 1–3 compared to the reference inhibitors (Table 1). The preliminary testing of the developed prodrugs showed that they exhibited very weak HDAC inhibitory activity compared to the corresponding parent inhibitors.

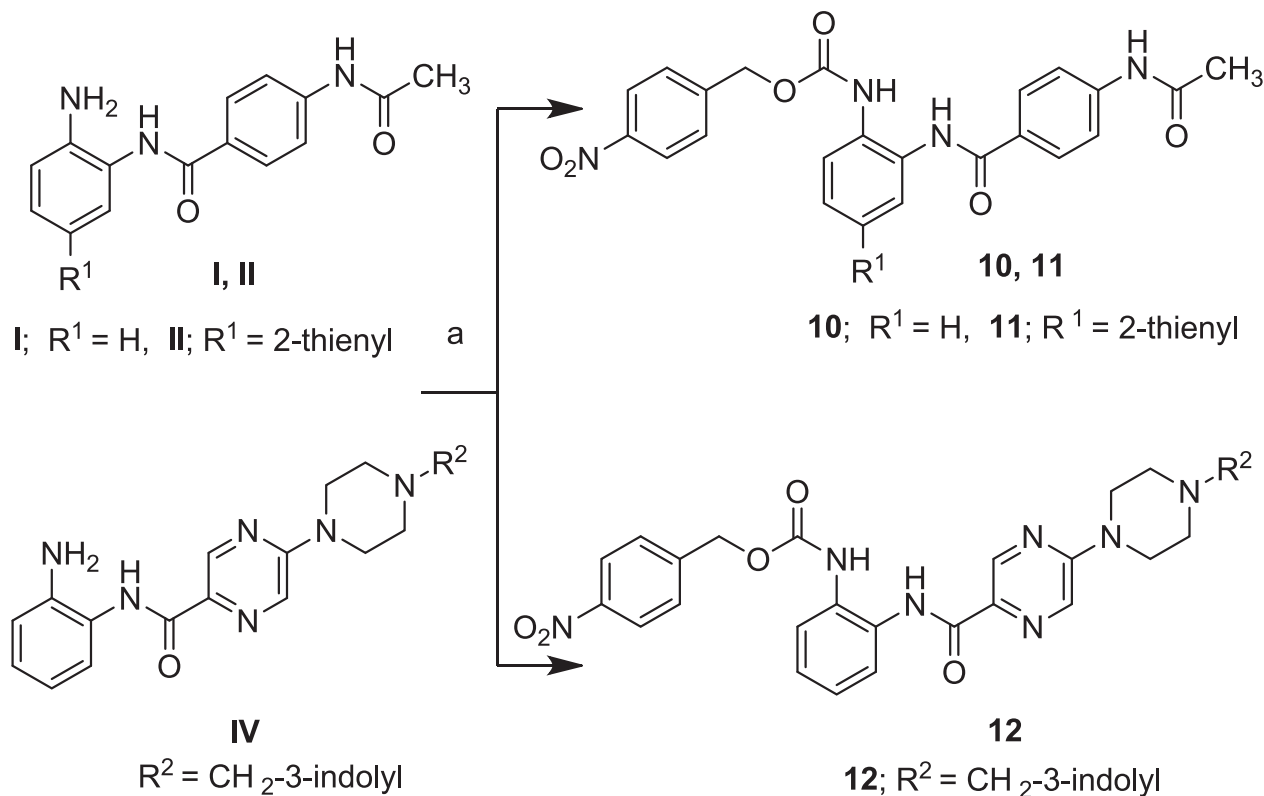
2.2.2 | Cellular testing

Cytotoxic activity against wild-type and NTR-THP1 cells

The prodrugs and their parent inhibitors were then tested in a cell viability assay via a tetrazolium salt-based assay on wild-type THP1 acute myeloid leukemia (AML) cells and THP1 cells that had been lentivirally transfected with the *E. coli* NTR NfsB. We had used this

system successfully before to activate bioreductive prodrugs of inhibitors of the lysine-specific demethylase 1 (LSD1).^[37] We pre-screened all compounds at 1, 10, and 50 μM concentrations in the wild-type and transfected cell lines (% inhibition against NTR-THP1 at 10 μM is presented in Table 1). When sub- μM inhibition of HDACs *in vitro* and more than 50% inhibition of cell viability were achieved by the prodrugs in the NTR-THP1 cells, a GI_{50} value was determined. For inhibitors **II** and **IV**, the more potent prodrugs **5** and **6**, respectively, were selected.

The two potent prodrugs **5** and **6** were both 2-nitroimidazole rather than nitrobenzyl compounds, which is in line with previous findings on the better activation of the heterocyclic prodrugs. Interestingly, compound **4** and compound **10** show little effect on NTR-THP1 cells at 10 μM (14% and 19% inhibition, Table 1), even so compound **4** is a nitroimidazole derivative. Potentially, the core structure (from compound **I**) is binding weakly to NTR and



SCHEME 2 Synthesis of 4-nitrobenzyl-based prodrugs **10–12**. Reagents and conditions: (a) 4-nitrobenzyl chloroformate (**9**), K₂CO₃, tetrahydrofuran (THF), RT, 4 h, 20%–33%.

subsequently prodrug activation is hindered. However, regarding compounds **5** and **6**, the cellular effects are in the range of the parent HDAC inhibitor, implying almost full conversion (Table 2). Whereas the parent HDAC inhibitors have essentially the same activity on both cell lines, we find a selectivity window of 6–12 fold for the prodrugs (Table 2). The inhibition in wild-type THP1 cells resulted either from the intrinsic toxicity of the carbamates or from some background reductive activation in the nontransfected cells. Thus, while the selectivity could still be improved, compound **6** is a prodrug with very good bio-reductive properties, which leads to highly potent activity against a leukemic cell line and is a great starting point for further optimization.

Cytotoxic activity against J774A.1 cells

To analyze the therapeutic window of the developed prodrugs, the cytotoxic properties of the prodrugs and the parent inhibitors were determined using a MTT assay protocol against the murine macrophage cell line (J774A.1) after incubation for 72 h. To quantify cytotoxic activity, the half-maximal inhibitory concentration (IC₅₀) was determined. The results, summarized in Figure 3 and Table 3, consistently showed that the synthesized prodrugs exhibited significantly higher IC₅₀ values compared to the corresponding parent HDAC inhibitors.

The ratio of prodrug IC₅₀ to parent compound IC₅₀ was calculated, revealing a 4- to 78-fold improvement in reducing cellular cytotoxicity

when using the prodrug approach instead of the parent HDAC inhibitors. Compounds **4** and **10** were found to be the least toxic prodrugs against J774A.1 cells. It was not possible to calculate accurate IC₅₀ values for both compounds as they demonstrated minimal or no cellular toxicity even at tested concentrations of up to 100 μM. At the same time, compounds **5** and **6** show moderate toxicity in J774A.1 cells, pointing towards potential off-target effects in this cell line.

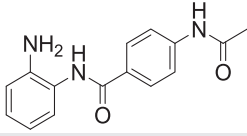
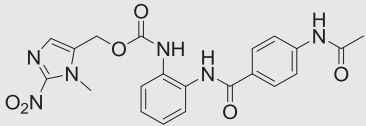
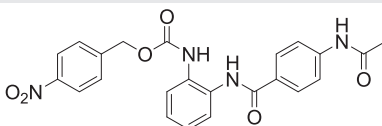
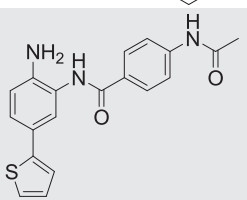
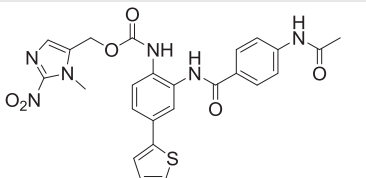
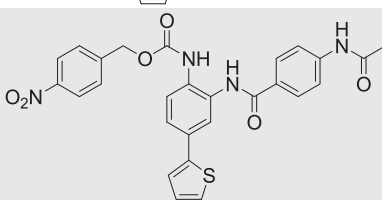
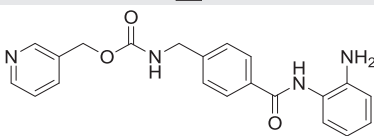
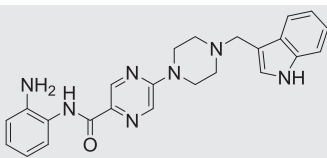
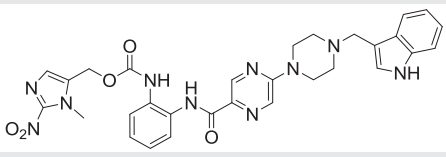
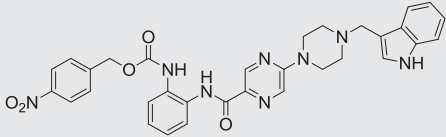
2.2.3 | In vitro prodrug activation by NTR

An liquid chromatography-mass spectrometry (LC-MS) analysis was performed to determine the interaction profile of the most promising prodrug **6** with *E. coli* NTR. After 30 min of incubation, the prodrug **6** (retention time: 5.6 min, *m/z*: 611.2473) reacted with NTR, resulting in the formation of the parent inhibitor (**IV**; retention time: 4.16 min, *m/z*: 428.2193), in addition to other metabolites (Figure 4, Table 4).

3 | CONCLUSION

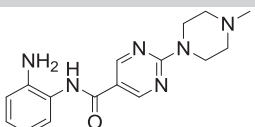
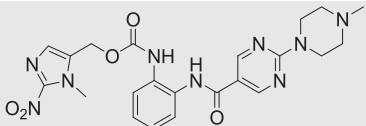
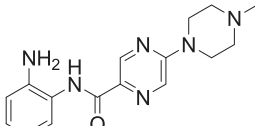
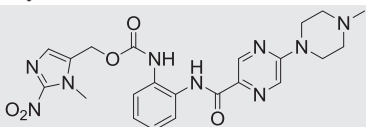
Over recent years, histone deacetylases (HDACs) have gained great interest as key epigenetic modulators involved in the regulation of several cellular processes, and their overexpression has been associated with the initiation and progression of

TABLE 1 In vitro evaluation of histone deacetylase (HDAC)1–3 inhibition by HDAC inhibitors I–VI and the corresponding prodrugs,^a in addition to % inhibition against nitroreductase (NTR)-THP1 at 10 μM.

Cpd. Id	Chemical structure	HDAC1, IC ₅₀ (μM) or % inhibition	HDAC2, IC ₅₀ (μM) or % inhibition	HDAC3, IC ₅₀ (μM) or % inhibition	% Inhibition NTR-THP1 at 10 μM
(I) ^b		8.8 ± 1.2	7.5 ± 0.8	4.2 ± 0.5	84
4		21% at 1 μM 8% at 0.1 μM	7% at 1 μM 2% at 0.1 μM	10% at 1 μM 12% at 0.1 μM	14
10		17% at 1 μM 10% at 0.1 μM	14% at 1 μM 8% at 0.1 μM	12% at 1 μM 7% at 0.1 μM	19
(II)		0.04 ± 0.006	0.26 ± 0.01	16.4 ± 3.6	88
5		31% at 1 μM 17% at 0.1 μM	8% at 1 μM 2% at 0.1 μM	11% at 1 μM 8% at 0.1 μM	98
11		14% at 1 μM 9% at 0.1 μM	7% at 1 μM 8% at 0.1 μM	9% at 1 μM 3% at 0.1 μM	35
(III)		0.93 ± 0.11	0.95 ± 0.03	1.8 ± 0.1	n.d. ^c
(IV)		0.13 ± 0.01	0.28 ± 0.01	0.31 ± 0.01	93
6		38% at 1 μM 16% at 0.1 μM	13% at 1 μM 3% at 0.1 μM	15% at 1 μM 11% at 0.1 μM	98
12		20% at 1 μM 12% at 0.1 μM	5% at 1 μM 1% at 0.1 μM	12% at 1 μM 5% at 0.1 μM	80

(Continues)

TABLE 1 (Continued)

Cpd. Id	Chemical structure	HDAC1, IC ₅₀ (μ M) or % inhibition	HDAC2, IC ₅₀ (μ M) or % inhibition	HDAC3, IC ₅₀ (μ M) or % inhibition	% Inhibition NTR- THP1 at 10 μ M
(V)		4.6 \pm 0.6	6.6 \pm 1.4	4.0 \pm 0.9	73
7		19% at 1 μ M 17% at 0.1 μ M	8% at 1 μ M 5% at 0.1 μ M	15% at 1 μ M 7% at 0.1 μ M	17
(VI)		1.1 \pm 0.3	6.2 \pm 0.8	5.2 \pm 1.1	88
8		25% at 1 μ M 20% at 0.1 μ M	10% at 1 μ M 1% at 0.1 μ M	16% at 1 μ M 9% at 0.1 μ M	93

^aAll experiments were conducted in triplicates.

^bThe codes for parent inhibitors are written in Latin numbers between brackets.

^cn.d. not determined.

different types of cancer. Several HDAC inhibitors have been approved for the treatment of different subtypes of blood malignancies; however, the majority of them show some limitations, including genotoxicity, mutagenicity, and undesirable adverse effects. One strategy that could be used to overcome such problems and improve drug delivery to selected cell types is the design of prodrugs. In the current study, a novel series of bioreductive nitroaromatic prodrugs for class I HDACs has been designed and synthesized based on different reported HDAC1–3 inhibitors. The aminobenzamide part (ZBG) of the selected HDAC inhibitors was masked with different nitroarylmethyl alcohols through a carbamate linker. Such attachments should reduce the binding to the targeted HDACs, which could be explained by the weaker HDAC inhibitory activity of the newly synthesized prodrugs compared to the parent inhibitors. Furthermore, the biological activity of the newly synthesized prodrugs was evaluated against THP1 acute myeloid leukemia cells using a NTR prodrug system. This prodrug system catalyzes the reduction of the nitro group of different nitroaromatic substrates of cytotoxic amines to release the active inhibitor selectively in NTR-expressing cells. Cellular testing revealed that two 2-nitroimidazole-based prodrugs (**5** and **6**) were activated by the NTR prodrug system. Both compounds showed cellular effects almost in the range of the corresponding parent inhibitors. Compound **6** showed potent activity against the NTR-THP1 cell in the nanomolar range. In addition, it exhibited a moderate selectivity window. The *in vitro* prodrug activation by NTR was confirmed by LC-MS analysis, which showed the release of the parent inhibitor after incubation of the prodrug **6** with *E. coli* NTR.

This work demonstrates that we successfully synthesized and evaluated a novel class I HDAC prodrug with good bioreductive properties, which can be used as a good starting point to enhance the selectivity and for further optimization. In addition, our model shows the potential to genetically engineer tumor cells with a bacterial NTR for specific activation.

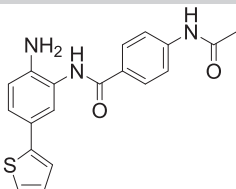
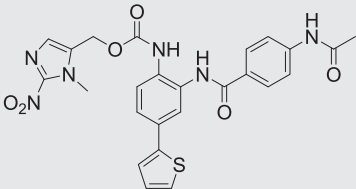
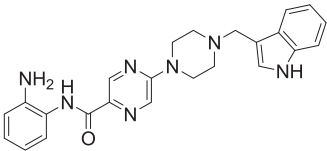
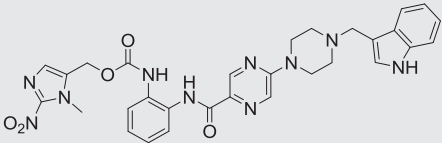
4 | EXPERIMENTAL

4.1 | Chemistry

4.1.1 | General

Materials and reagents were purchased from Sigma-Aldrich Co., Ltd. and abcr GmbH (Karlsruhe). All solvents were analytically pure and dried before use. Thin-layer chromatography was carried out on aluminum sheets coated with silica gel 60 F254 (Merck). For medium-pressure chromatography (MPLC), silica gel 60 (0.036–0.200 mm) was used. Purity was measured by UV absorbance at 254 nm. The elution system used for high-performance liquid chromatography (HPLC) consists of MeOH, H₂O, and 0.05% trifluoroacetic acid. The HPLC consisted of a LiChrosorb[®] RP-18 (5 μ m) 100–4.6 Merck column (Merck), two LC-10AD pumps, a SPD-M10A VP PDA detector, and a SIL-HT autosampler, all from the manufacturer Shimadzu. The absorption spectra were recorded with a Shimadzu SPD-M10A diode array detector spectrophotometer. For the preparative HPLC, a LiChrosorb[®] RP-18 (7 μ m) 250–25 Merck column was used. The applied mobile phase was a gradient with increasing polarity composed of acetonitrile/water and formic acid. Mass

TABLE 2 GI₅₀ values of the most active prodrugs and the corresponding inhibitors against wild-type and transfected nitroreductase (NTR)-THP1 cells and their selectivity window.^a

Cpd. Id	Chemical structure	Inhibition of viability in THP1 cells, IC ₅₀ (μM) ± SEM	Inhibition of viability in NTR-THP1 cells, IC ₅₀ (μM) ± SEM	Selectivity window
(II)		1.67 ± 0.51	1.62 ± 0.62	1.0
5		12.3 ± 0.7	1.84 ± 0.4	6.7
(IV)		0.034 ± 0.003	0.063 ± 0.013	0.5
6		0.91 ± 0.36	0.077 ± 0.004	11.8

^aAll experiments were conducted in triplicates.

spectrometry (MS) analyses were performed with a Finnigan MAT710C (Thermo Separation Products) for the ESI MS spectra and with a LTQ (linear ion trap) Orbitrap XL hybrid mass spectrometer (Thermo Fisher Scientific) for the HRMS-ESI (high-resolution mass spectrometry) spectra. For the HRMS analyses, the signal for the isotopes with the highest prevalence was given and calculated. ¹H NMR spectra (see the Supporting Information) were taken on a Varian Inova 400 using deuterated DMSO as solvent. Chemical shifts were referenced to the residual solvent signals. The following abbreviations and formulas for solvents and reagents were used: ethyl acetate (EtOAc), *N,N*-dimethylformamide (DMF), dimethyl sulfoxide (DMSO), methanol (MeOH), tetrahydrofuran (THF), water (H₂O), sodium sulphate (Na₂SO₄), dichloromethane (DCM), potassium carbonate (K₂CO₃), and HOBt.

Intermediate 1 and the aniline derivatives I–II and IV–VI were synthesized according to the previously reported methods^[37] and^[18,19,40], respectively.

The InChI codes of the investigated compounds, together with some biological activity data, are provided as Supporting Information.

4.1.2 | Synthesis of (1-methyl-2-nitro-1*H*-imidazol-5-yl)methyl 4-nitrophenyl carbonate 3

4-Nitrophenyl chloroformate (2) (492 mg, 2.44 mmol, 1.2 eq.) in dry THF (5 mL) was added slowly to an ice-cold solution of intermediate 1 (320 mg, 2.37 mmol, 1 eq.) in dry THF (15 mL) and pyridine (0.2 mL,

2.44 mmol, 1.2 eq.). The reaction was allowed to warm to room temperature and stirred overnight. The reaction mixture was evaporated to dryness, EtOAc was added, and the solution was washed with HCl (1 M, 15 mL) and brine (15 mL). The combined organic layers were dried over Na₂SO₄, filtered, and concentrated under reduced pressure. The crude product was purified by MPLC (EtOAc/hexane) to give the product as white solid (yield: 220 mg, 0.68 mmol, 33.8%); ¹H NMR (400 MHz, DMSO-*d*₆) δ 8.32 (d, *J* = 9.1 Hz, 2H), 7.57 (d, *J* = 9.1 Hz, 2H), 7.35 (s, 1H), 5.45 (s, 2H), 3.97 (s, 3H).

4.1.3 | General procedure for the synthesis of compounds 4–8

(1-Methyl-2-nitro-1*H*-imidazol-5-yl)methyl (4-nitrophenyl) carbonate (3) (100 mg, 0.31 mmol, 1 eq.) was added to a mixture of HOBt·H₂O (60 mg, 0.39 mmol, 1.3 eq.) and the appropriate aniline derivative (I, II, IV–VI) (0.31 mmol, 1 eq.) in dry DMF (5 mL), and the resulting reaction mixture was stirred at RT for 18 h. The solvent was removed under reduced pressure. The crude product was purified by MPLC using (DCM/MeOH) to give the corresponding final product.

(1-Methyl-2-nitro-1*H*-imidazol-5-yl)methyl *N*-[2-(4-acetamidobenzamido)phenyl]carbamate (4): ¹H NMR (400 MHz, DMSO-*d*₆) δ 10.20 (s, 1H), 9.72 (s, 1H), 9.00 (s, 1H), 7.89 (d, *J* = 8.8 Hz, 2H), 7.69 (d, *J* = 8.8 Hz,

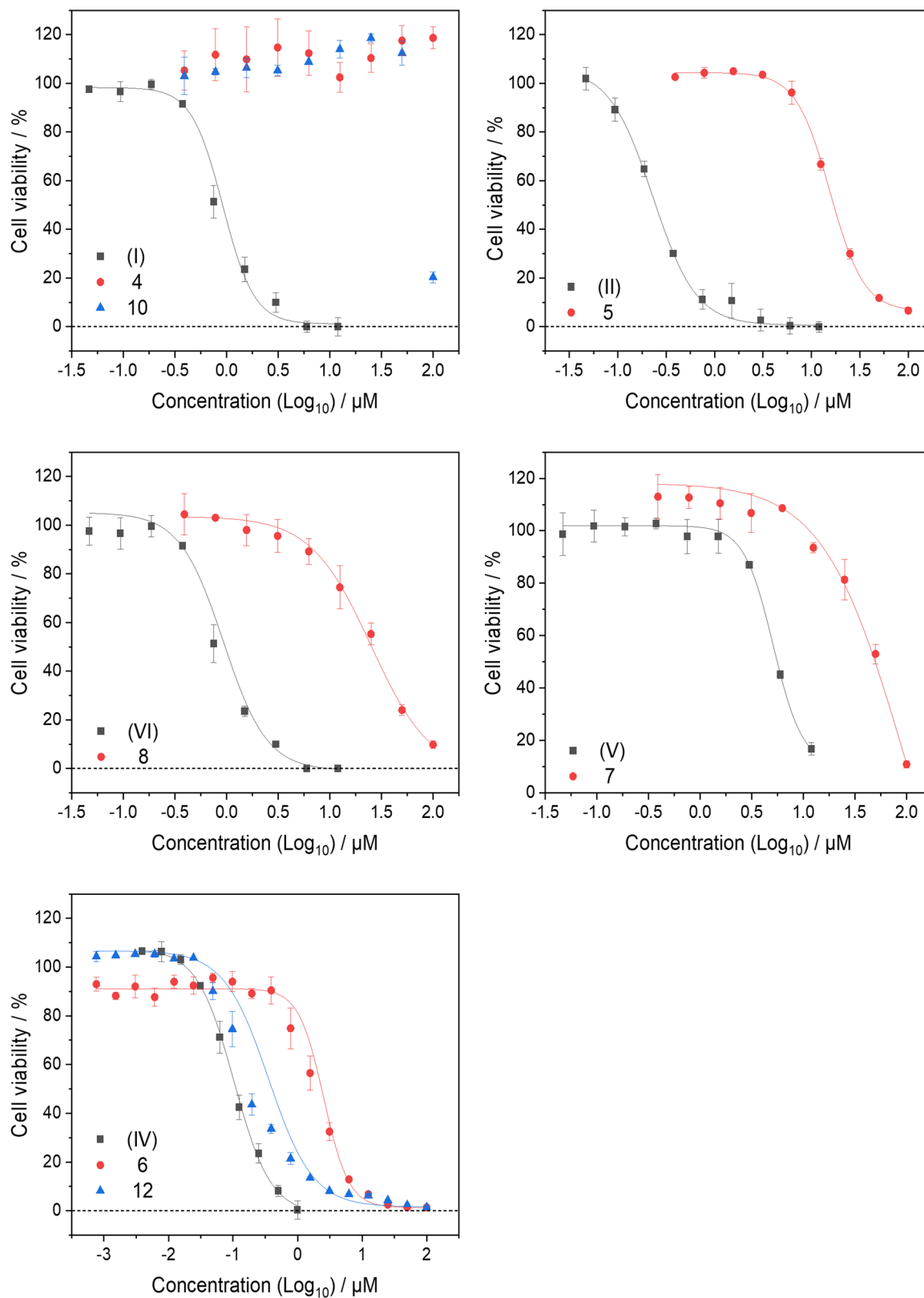


FIGURE 3 Dose–response curves against J774A.1 cell line showing cytotoxic activities of histone deacetylase (HDAC) inhibitors and corresponding prodrugs.

TABLE 3 IC₅₀ values for histone deacetylase (HDAC) inhibitors and corresponding prodrugs against J774A.1 cells for a 72-h incubation period were determined in the MTT assay.^a

Cpd. Id	IC ₅₀ (μM) ± SEM	Prodrug to parent inhibitor, IC ₅₀ ratio
(I)	0.9 ± 0.7	NA
4	NA	NA
10	NA	NA
(II)	0.2 ± 0.02	NA
5	15.5 ± 0.6	77.5
(IV)	0.1 ± 0.05	NA
6	2.5 ± 0.6	25
12	0.4 ± 0.04	4
(V)	5.1 ± 0.2	NA
7	61.9 ± 0.5	12.1
(VI)	0.8 ± 0.3	NA
8	23.3 ± 3.7	29.1

^aAll experiments were conducted in triplicates.

2H), 7.56 (d, *J* = 7.6 Hz, 1H), 7.50 (dd, *J* = 7.8, 1.6 Hz, 1H), 7.27 (s, 1H), 7.23–7.14 (m, 2H), 5.25 (s, 2H), 3.90 (s, 3H), 2.06 (s, 3H); ¹³C NMR (101 MHz, DMSO-*d*₆) δ 169.2, 165.4, 153.8, 142.9, 133.7, 131.8, 130.73, 130.71, 129.19, 129.13, 128.8, 126.6, 126.0, 125.0, 118.5, 55.9, 34.6, 24.6; HRMS *m/z*: 475.1336 [M+Na]⁺; calculated C₂₁H₂₀N₆O₆Na⁺: 475.1342; HPLC: rt 9.82 min (98.83%); white solid; yield: 90 mg, 0.2 mmol, 64.3%.

(1-Methyl-2-nitro-1*H*-imidazol-5-yl)methyl *N*-[2-(4-acetamidobenzamido)-4-(thiophen-2-yl)phenyl]carbamate (5): ¹H NMR (400 MHz, DMSO-*d*₆) δ 10.21 (s, 1H), 9.81 (s, 1H), 9.10 (s, 1H), 7.92 (d, *J* = 8.8 Hz, 2H), 7.80 (d, *J* = 2.2 Hz, 1H), 7.71 (d, *J* = 8.8 Hz, 2H), 7.63 (d, *J* = 8.5 Hz, 1H), 7.56–7.50 (m, 2H), 7.45 (dt, *J* = 3.6, 1.9 Hz, 1H), 7.28 (s, 1H), 7.11 (dt, *J* = 7.9, 4.0 Hz, 1H), 5.26 (s, 2H), 3.92 (s, 3H), 2.07 (s, 3H); ¹³C NMR (101 MHz, DMSO-*d*₆) δ 169.2, 165.6, 153.8, 146.5, 143.0, 142.9, 133.6, 131.3, 131.0, 130.98, 130.54, 129.2, 129.0, 128.7, 126.0, 124.0, 123.3, 123.1, 118.5, 56.0, 34.7, 24.6; HRMS *m/z*: 557.1215 [M+Na]⁺; calculated C₂₅H₂₂N₆O₆SNa⁺: 557.1219; HPLC: rt 12.60 min (97.29%); white solid; yield: 75 mg, 0.14 mmol, 45.2%.

(1-Methyl-2-nitro-1*H*-imidazol-5-yl)methyl *N*-[2-(5-{4-[(1*H*-indol-3-yl)methyl]piperazin-1-yl}pyrazine-2-amido)phenyl]carbamate (6): ¹H

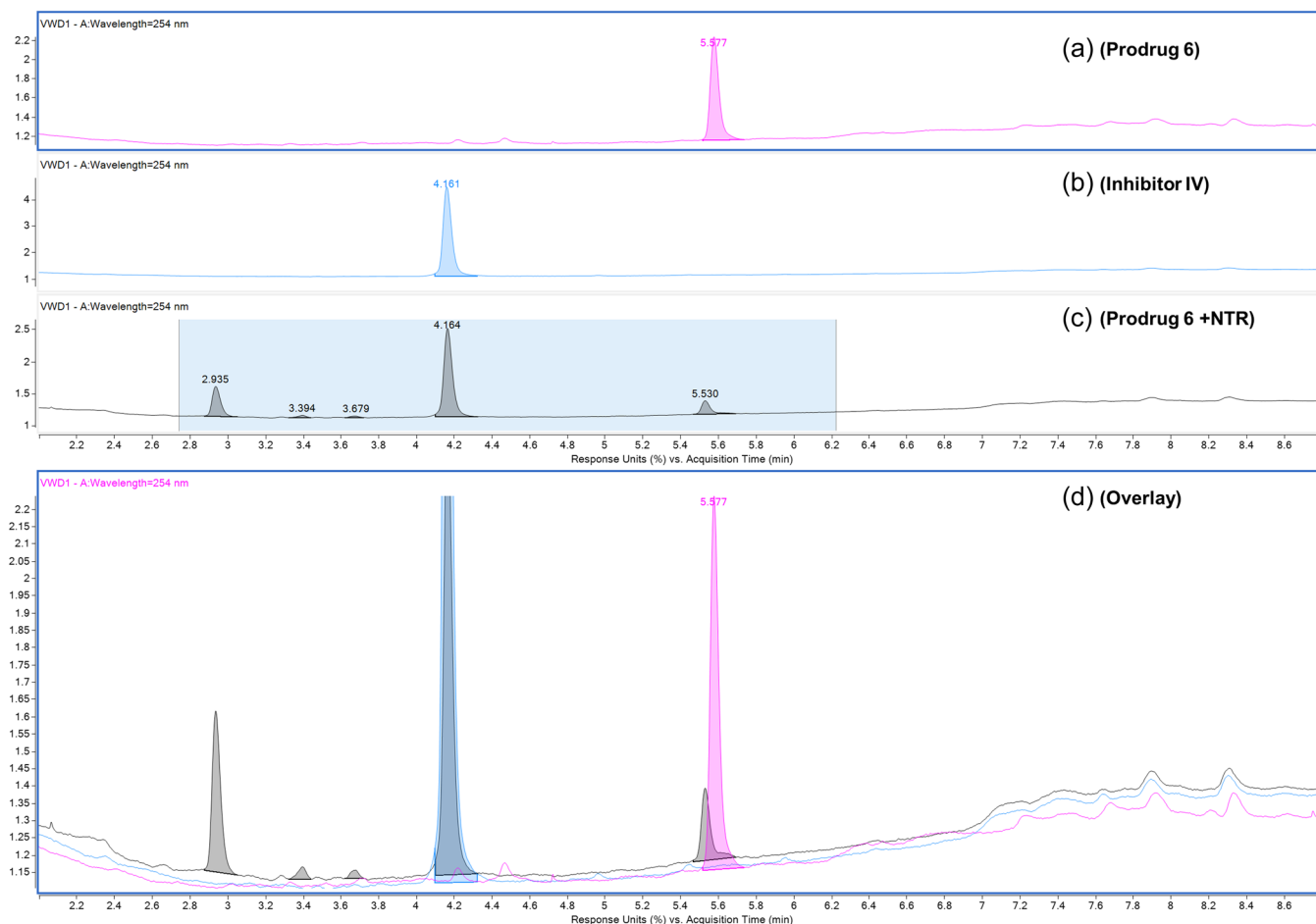


FIGURE 4 HPLC chromatogram of the reduction reaction for prodrug 6 catalyzed by nitroreductase (NTR) at a 30-min reaction time. (a) Chromatogram of 6 without NTR; (b) chromatogram of the parent inhibitor IV; (c) chromatogram of 6 with NTR showing the release of the inhibitor IV; (d) overlay of the three chromatograms. HPLC, high-performance liquid chromatography.

TABLE 4 LC-MS of prodrug **6** activated by nitroreductase (NTR).

	Retention time (min)	<i>m/z</i>
Prodrug 6	5.58	611.2473
Parent HDAC inhibitor IV	4.16	428.2193
Prodrug 6 with NTR	2.95	466.1944
	4.16	428.2193
	5.55	611.2471

NMR (400 MHz, DMSO-*d*₆) δ 10.93 (s, 1H), 9.83 (s, 1H), 9.40 (s, 1H), 8.67 (s, 1H), 8.24 (s, 1H), 7.95 (d, *J* = 15.2 Hz, 1H), 7.66 (d, *J* = 7.8 Hz, 1H), 7.50–7.20 (m, 5H), 7.14 (t, *J* = 7.6 Hz, 1H), 7.06 (t, *J* = 7.3 Hz, 1H), 6.98 (t, *J* = 7.4 Hz, 1H), 5.28 (s, 2H), 3.90 (s, 3H), 3.79–3.60 (m, 6H), 2.62–2.50 (m, 4H); ¹³C NMR (101 MHz, DMSO-*d*₆) δ 161.7, 155.1, 153.9, 142.3, 142.2, 136.3, 133.3, 131.7, 128.83, 128.80, 128.7, 127.6, 126.0, 124.7, 124.6, 124.5, 121.0, 119.0, 118.4, 111.3, 110.4, 55.5, 53.0, 52.0, 44.0, 34.2; HRMS *m/z*: 611.2476 [M+H]⁺; calculated C₃₀H₃₁N₁₀O₅⁺: 611.2479; HPLC: rt 11.16 min (99.75%); beige solid; yield: 50 mg, 0.08 mmol, 26.3%.

(1-Methyl-2-nitro-1*H*-imidazol-5-yl)methyl *N*-[2-(4-methylpiperazin-1-yl)pyrimidine-5-amido]phenyl]carbamate (**7**): ¹H NMR (400 MHz, DMSO-*d*₆) δ 9.68 (s, 1H), 9.04 (s, 1H), 8.84 (s, 2H), 7.60 (d, *J* = 16.6 Hz, 1H), 7.48 (dd, *J* = 7.9, 1.5 Hz, 1H), 7.26 (s, 1H), 7.21 (td, *J* = 7.7, 1.6 Hz, 1H), 7.15 (td, *J* = 7.6, 1.5 Hz, 1H), 5.25 (s, 2H), 3.91 (s, 3H), 3.84 (t, *J* = 5.0 Hz, 4H), 2.40 (t, *J* = 5.0 Hz, 4H), 2.24 (s, 3H); ¹³C NMR (101 MHz, DMSO-*d*₆) δ 163.4, 161.8, 158.6, 158.5, 153.8, 133.7, 132.1, 129.2, 126.7, 126.1, 116.4, 55.9, 54.7, 46.1, 43.9, 34.6; HRMS *m/z*: 496.205 [M+H]⁺; calculated C₂₂H₂₆N₉O₅⁺: 496.205; HPLC: rt 8.58 min (92.05%); colorless oil; Yield: 35 mg, 0.07 mmol, 22.9%.

(1-Methyl-2-nitro-1*H*-imidazol-5-yl)methyl *N*-[2-[5-(4-methylpiperazin-1-yl)pyrazine-2-amido]phenyl]carbamate; formic acid (**8**): ¹H NMR (400 MHz, DMSO-*d*₆) δ 9.86 (s, 1H), 9.42 (s, 1H), 8.69 (d, *J* = 1.1 Hz, 1H), 8.27 (s, 1H), 7.97 (s, 1H), 7.89 (d, *J* = 8.4 Hz, 1H), 7.60 (d, *J* = 8.3 Hz, 1H), 7.46–7.38 (m, 1H), 7.35–7.29 (m, 1H), 7.27–7.21 (m, 1H), 7.15 (td, *J* = 7.7, 1.3 Hz, 1H), 5.29 (s, 2H), 3.90 (s, 3H), 3.79–3.62 (m, 4H), 2.55–2.49 (m, 4H), 2.30 (s, 3H); HRMS *m/z*: 496.205 [M+H]⁺; calculated C₂₂H₂₆N₉O₅⁺: 496.205. The compound exists as formic acid salt as it was purified using preparative HPLC; HPLC: rt 9.17 min (97.95%); colorless oil; yield: 20 mg.

4.1.4 | General procedure for the synthesis of compounds **10–12**

A solution of 4-nitrobenzyl chloroformate (**9**) (100 mg, 0.46 mmol, 1 eq.) in 3 mL of THF was added dropwise to a mixture of the appropriate aniline derivative (**I–III**) (0.46 mmol, 1 eq.) and K₂CO₃ (83 mg, 0.6 mmol, 1.3 eq.) in dry THF (10 mL) at 0°C. The reaction mixture was stirred at rt for 4 h. The reaction mixture was filtered, and the solvent was evaporated under reduced pressure. The

obtained residue was purified using MPLC (DCM/MeOH) to give the corresponding product.

(4-Nitrophenyl)methyl *N*-[2-(4-acetamidobenzamido)phenyl]carbamate (**10**): ¹H NMR (400 MHz, DMSO-*d*₆) δ 10.20 (s, 1H), 9.73 (s, 1H), 9.13 (s, 1H), 8.20–8.14 (m, 2H), 7.92–7.86 (m, 2H), 7.68 (d, *J* = 8.8 Hz, 2H), 7.62 (d, *J* = 8.8 Hz, 2H), 7.56 (dd, *J* = 7.8, 1.5 Hz, 1H), 7.51 (dd, *J* = 7.7, 1.7 Hz, 1H), 7.24–7.13 (m, 2H), 5.27 (s, 2H), 2.06 (s, 3H); ¹³C NMR (101 MHz, DMSO-*d*₆) δ 169.2, 165.4, 154.2, 147.4, 145.0, 142.9, 131.9, 130.8, 129.1, 128.8, 128.7, 127.5, 126.6, 126.0, 125.0, 124.0, 118.5, 65.2, 24.6; HRMS *m/z*: 471.1274 [M+Na]⁺; calculated C₂₃H₂₀N₄O₆Na⁺: 471.1280; HPLC: rt 11.66 min (95.69%); white solid; yield: 65 mg, 0.14 mmol, 32.5%.

(4-Nitrophenyl)methyl *N*-[2-(4-acetamidobenzamido)-4-(thiophen-2-yl)phenyl]carbamate (**11**): ¹H NMR (400 MHz, DMSO-*d*₆) δ 10.21 (s, 1H), 9.81 (s, 1H), 9.20 (s, 1H), 8.18 (d, *J* = 8.8 Hz, 2H), 7.92 (d, *J* = 8.7 Hz, 2H), 7.79 (d, *J* = 2.1 Hz, 1H), 7.69 (d, *J* = 8.7 Hz, 2H), 7.66–7.60 (m, 3H), 7.55–7.49 (m, 2H), 7.45 (dd, *J* = 3.6, 1.0 Hz, 1H), 7.11 (dd, *J* = 5.1, 3.6 Hz, 1H), 5.29 (s, 2H), 2.07 (s, 3H); ¹³C NMR (101 MHz, DMSO-*d*₆) δ 169.2, 165.6, 154.2, 147.5, 144.9, 143.0, 142.96, 131.4, 131.0, 130.5, 129.2, 129.0, 128.8, 128.6, 127.5, 126.0, 124.0, 123.7, 123.4, 123.1, 118.5, 65.3, 24.6; HRMS *m/z*: 553.1153 [M+Na]⁺; calculated C₂₇H₂₂N₄O₆Na⁺: 553.1158; HPLC: rt 13.78 min (95.31%); white solid; yield: 72 mg, 0.14 mmol, 28.8%.

(4-Nitrophenyl)methyl *N*-[2-(5-{4-[(1*H*-indol-3-yl)methyl]piperazin-1-yl}pyrazine-2-amido)phenyl]carbamate (**12**): ¹H NMR (400 MHz, DMSO-*d*₆) δ 10.93 (s, 1H), 9.88 (s, 1H), 9.48 (s, 1H), 8.68 (d, *J* = 1.3 Hz, 1H), 8.19–8.09 (m, 3H), 7.94 (s, 1H), 7.68–7.57 (m, 3H), 7.34 (d, *J* = 8.0 Hz, 2H), 7.26–7.21 (m, 2H), 7.15 (td, *J* = 7.7, 1.5 Hz, 1H), 7.09–7.03 (m, 1H), 7.00–6.95 (m, 1H), 5.29 (s, 2H), 3.69 (s, 6H), 2.56–2.50 (m, 4H); ¹³C NMR (101 MHz, DMSO-*d*₆) δ 162.2, 156.3, 155.5, 154.8, 150.4, 147.4, 145.0, 142.7, 136.8, 132.2, 129.2, 128.7, 128.0, 126.4, 126.3, 125.2, 125.1, 125.06, 123.9, 121.4, 119.5, 118.9, 111.8, 110.8, 65.3, 53.5, 52.5, 44.5; HRMS *m/z*: 607.2412 [M+H]⁺; calculated C₃₂H₃₁N₈O₅⁺: 607.2417; HPLC: rt 11.87 min (97.29%); beige solid; yield: 55 mg, 0.09 mmol, 19.57%.

4.2 | Biological assays

4.2.1 | In vitro HDAC inhibition assay

Recombinant human proteins HDAC1–3/NCOR1 were purchased from ENZO Life Sciences AG (Lausen, CH). The in vitro testing on recombinant HDACs 1–3 was performed with a fluorogenic peptide derived from p53 (Ac-RHKK(Acetyl)-AMC) as reported.^[18] The measurements were performed in assay buffer (50 mM Hepes, 150 mM NaCl, 5 mM MgCl₂, 1 mM TCEP, and 0.2 mg/mL BSA, pH 7.4 adjusted with NaOH) at 37°C. All compounds at different concentrations were incubated with 10 nM HDAC1, 3 nM HDAC2, or 3 nM HDAC3 (final concentration) for at least 5 min. The reaction was first started with the addition of a fluorogenic peptide substrate (20 μM final concentration) and incubated for 30 min for HDAC2 and 3 and 90 min for HDAC1. The reaction was then stopped

with a solution of 1 mg/mL trypsin and 20 μM SAHA in 1 mM HCl and incubated for 1 h at 37°C. The fluorescence intensity was measured with an Envision 2104 Multilabel Plate Reader (PerkinElmer) with an excitation wavelength of 380 ± 8 nm and an emission wavelength of 430 ± 8 nm. The measured fluorescence intensities were normalized with uninhibited reaction as 100% and the reaction without enzyme as 0%. A nonlinear regression analysis was done to determine the IC_{50} value.

4.2.2 | Cellular testing

Cytotoxic activity against wild-type THP1 and NTR-THP1 cells

The NTR-expressing cell line THP1-NTR was generated in the group of Prof. Miething from the University of Freiburg Medical Center, by lentiviral transfection of wild-type THP1 cells (RRID:CVCL_0006), which was a kind gift of Prof. Lübbert from the University Hospital, Freiburg, with an nfsb gene construct. Both cell lines were cultivated in RPMI1640 medium supplemented with 10% (v/v) FCS, 2 mM L-glutamine and 1% penicillin/streptomycin at 37°C in a humidified atmosphere with 5% CO_2 . Cells were diluted to 5×10^4 cells mL^{-1} , and mixed with compounds to a final DMSO concentration of 0.5% and seeded at 100 μL in 96-well plates in triplicates. After 72 h incubation, the CellTiter 96[®] AQueous Nonradioactive Cell Proliferation Assay from Promega was performed according to the manufacturer's instructions. Assay plates were measured at 492 nm on a POLARstar Optima microplate reader (BMG Labtech, Germany). Data were plotted as absorbance units against the logarithm of compound concentration using OriginPro 9G (OriginLab). Fifty percent inhibition of viability (GI_{50}) was determined as compound concentration required to reduce the number of metabolic active cells by 50% compared to DMSO control. The assay had already been described.^[37]

Cytotoxic activity against J774A.1 cell line

Murine macrophage cell line J774A.1 was maintained under standard conditions at 37°C and 5% CO_2 in DMEM (high glucose) supplemented with 10% fetal bovine serum.

Cytotoxic properties of active drugs. Cytotoxic properties of active drugs were determined in MTT assay against J774A.1 cells. 2000 cells/well were plated in 96 well plates. Cells were incubated overnight and the medium was removed from assay wells. Subsequently, 100 μL of compounds **I**, **II**, **V**, and **VI** were applied to cells at concentrations of 12, 6, 3, 1.5, 0.75, 0.375, 0.187, 0.094, 0.047 μM , while compound **IV** was applied at concentrations of 1, 0.5, 0.25, 0.125, 0.0625, 0.0313, 0.0156, 0.0078, 0.0039 μM . DMSO at concentration 0.2% (v/v) was used as vehicle control. After 72 h incubation MTT assay was performed. All experiments were conducted in triplicate and repeated at least twice.

Cytotoxic properties of prodrugs. Cytotoxic properties of prodrugs are determined in MTT assay against J774A.1 cells. 2000 cells/well were plated in 96 well plates. Cells were incubated overnight and the medium was removed from assay wells. Subsequently, 100 μL of prodrugs 4, 5, 7, 8, and 10 were applied to cells at

concentrations of 100, 50, 25, 12.5, 6.3, 3.1, 1.6, 0.8, 0.4, and 100 μL of prodrugs 6 and 12 at concentrations of 100, 50, 25, 12.5, 6.25, 3.125, 1.563, 0.781, 0.391, 0.195, 0.098, 0.049, 0.024, 0.012, 0.006, 0.003, 0.002, 0.0001 μM . DMSO at concentration 0.5% (v/v) was used as vehicle control. After 72 h incubation MTT assay was performed. All experiments were conducted in triplicate and repeated at least twice.

MTT assay. At designated time point medium in assay wells of 96-well cell culture plates was replaced with equal volume (100 μL) of the 0.5 mg/mL MTT solution in phenol free complete culture medium. The plates were incubated for 3 h at 37°C, 5% CO_2 . Upon incubation the medium was carefully removed and formazan crystals were solubilized with 100 μL DMSO for 10 min on orbital shaker at 300 rpm. Absorbance was measured with Tecan Spark 10 M microplate reader (Tecan Trading AG) at 500 nm and a reference wavelength of 650 nm. The percentage of cell viability was determined using the following formula: $(\text{OD}_{500} \text{ sample}/\text{OD}_{500} \text{ control}) \times 100$.

4.2.3 | In vitro prodrug activation by NTR

In vitro prodrug activation by NTR was performed with an assay mixture containing final concentrations: 200 μM of 6, 1.5 mM NADH, 1.5 μM FMN, and 250 nM NTR. Reactions were carried out in HEPES buffer (50 mM, pH 7.4) containing 2.5% DMSO as co-solvent at 37°C for 30 min at 300 rpm. At designated time aliquots from control and reaction samples were collected and the reaction was stopped by mixing 1:1 with cold acetonitrile (ACN). Chromatographic separation was achieved using an ACQUITY UPLC BEH C18 Column (130 \AA , 1.7 μm , 2.1 mm \times 100 mm). Mobile phase A consisted of water supplemented with 0.1% formic acid (FA) and mobile phase B consisted of ACN supplemented with 0.1% FA. Analysis was performed with a flow rate of 0.5 mL/min using the following program: 0–12 min gradient of 10%–80% mobile phase B, 12–14 min at 100% mobile phase B. Column temperature was maintained at 50°C. The mass spectrophotometry study was performed with Agilent 6546 LC/Q-TOF operating in the positive ion mode.

ACKNOWLEDGMENTS

This study was supported by the Excellence Strategy of the German Federal and State Governments (CIBSS–EXC 2189), to Manfred Jung, Mariia Zmyslia, and Claudia Jessen-Trefzger acknowledge support by Deutsche Forschungsgemeinschaft (DFG) grant 278002225/RTG 2202. Mohamed Abdelsalam, Sebastian Hilscher, and Wolfgang Sippl acknowledge support by the Deutsche Forschungsgemeinschaft (DFG) grants 469954457 and 471614207. Hany S. Ibrahim was funded by the Alexander von Humboldt Foundation Project EGY 1191187. Mohamed Abdelsalam appreciates the support of DAAD and the Ministry of Higher Education and Scientific Research (Egypt) through the GERLS scholarship. Open Access funding enabled and organized by Projekt DEAL.

CONFLICTS OF INTEREST STATEMENT

The authors declare no conflicts of interest.

ORCID

Mohamed Abdelsalam  <https://orcid.org/0000-0001-6559-2527>

Sebastian Hilscher  <http://orcid.org/0009-0003-0611-7365>

Hany S. Ibrahim  <https://orcid.org/0000-0002-1048-4059>

Mike Schutkowski  <https://orcid.org/0000-0003-0919-7076>

Manfred Jung  <https://orcid.org/0000-0002-6361-7716>

Claudia Jessen-Trefzer  <https://orcid.org/0000-0003-4216-8189>

Wolfgang Sippl  <http://orcid.org/0000-0002-5985-9261>

REFERENCES

- [1] J. Fan, K. A. Krautkramer, J. L. Feldman, J. M. Denu, *ACS Chem. Biol.* **2015**, *10*, 95.
- [2] A. J. Bannister, T. Kouzarides, *Cell Res.* **2011**, *21*, 381.
- [3] X. J. Sun, N. Man, Y. Tan, S. D. Nimer, L. Wang, *Front. Oncol.* **2015**, *5*, 108.
- [4] E. Seto, M. Yoshida, *Cold Spring Harbor Perspect. Biol.* **2014**, *6*, a018713.
- [5] S.-Y. Park, J.-S. Kim, *Exp. Mol. Med.* **2020**, *52*, 204.
- [6] K. Pant, E. Peixoto, S. Richard, S. A. Gradilone, *Cells* **2020**, *9*, 780.
- [7] S. Roperio, M. Esteller, *Mol. Oncol.* **2007**, *1*, 19.
- [8] M. J. Lee, Y. S. Kim, S. K. Kimm, G. Giaccone, J. B. Trepel, *Curr. Opin. Oncol.* **2008**, *20*, 639.
- [9] S. D. Pramanik, A. Kumar Halder, U. Mukherjee, D. Kumar, Y. N. Dey, *Front. Chem.* **2022**, *10*, 948217.
- [10] I.-C. Chen, B. Sethy, J.-P. Liou, *Front. Cell. Dev. Biol.* **2020**, *8*, 576391.
- [11] L. Zhang, J. Zhang, Q. Jiang, L. Zhang, W. Song, *J. Enzyme Inhib. Med. Chem.* **2018**, *33*, 714.
- [12] F. F. Wagner, M. Weiwer, M. C. Lewis, E. B. Holson, *Neurotherapeutics* **2013**, *10*, 589.
- [13] J. Melesina, C. V. Simoben, L. Praetorius, E. F. Bülbül, D. Robaa, W. Sippl, *ChemMedChem* **2021**, *16*, 1336.
- [14] C. J. Vickers, C. A. Olsen, L. J. Leman, M. R. Ghadiri, *ACS Med. Chem. Lett.* **2012**, *3*, 505.
- [15] J. Perrin, T. Werner, N. Kurzawa, A. Rutkowska, D. D. Childs, M. Kalxdorf, D. Poekkel, E. Stonehouse, K. Strohmmer, B. Heller, D. W. Thomson, J. Krause, I. Becher, H. C. Eberl, J. Vappiani, D. C. Sevin, C. E. Rau, H. Franken, W. Huber, M. Faelth-Savitski, M. M. Savitski, M. Bantscheff, G. Bergamini, *Nat. Biotechnol.* **2020**, *38*, 303.
- [16] I. Becher, T. Werner, C. Doce, E. A. Zaal, I. Tögel, C. A. Khan, A. Rueger, M. Muelbaier, E. Salzer, C. R. Berkens, P. F. Fitzpatrick, M. Bantscheff, M. M. Savitski, *Nat. Chem. Biol.* **2016**, *12*, 908.
- [17] S. Shen, A. P. Kozikowski, *ChemMedChem* **2016**, *11*, 15.
- [18] H. S. Ibrahim, M. Abdelsalam, Y. Zeyn, M. Zessin, A. M. Mustafa, M. A. Fischer, P. Zeyn, P. Sun, E. F. Bulbul, A. Vecchio, F. Erdmann, M. Schmidt, D. Robaa, C. Barinka, C. Romier, M. Schutkowski, O. H. Kramer, W. Sippl, *Int. J. Mol. Sci.* **2021**, *23*, 369.
- [19] O. M. Moradei, T. C. Mallais, S. Frechette, I. Paquin, P. E. Tessier, S. M. Leit, M. Fournel, C. Bonfils, M.-C. Trachy-Bourget, J. Liu, T. P. Yan, A.-H. Lu, J. Rahil, J. Wang, S. Lefebvre, Z. Li, A. F. Vaisburg, J. M. Besterman, *J. Med. Chem.* **2007**, *50*, 5543.
- [20] S. Subramanian, S. E. Bates, J. J. Wright, I. Espinoza-Delgado, R. L. Piekarz, *Pharmaceuticals* **2010**, *3*, 2751.
- [21] O. Bruserud, C. Stapnes, E. Ersvæ, B. Gjertsen, A. Rynningen, *Curr. Pharm. Biotechnol.* **2007**, *8*, 388.
- [22] X. Gao, L. Shen, X. Li, J. Liu, *Exp. Ther. Med.* **2019**, *18*, 1057.

- [23] W. Fan, L. Zhang, Q. Jiang, W. Song, F. Yan, L. Zhang, *Eur. J. Med. Chem.* **2020**, *203*, 112628.
- [24] D. Jornada, G. dos Santos Fernandes, D. Chiba, T. de Melo, J. dos Santos, M. Chung, *Molecules* **2015**, *21*, 42.
- [25] C. Karnthaler-Benbakka, D. Groza, B. Koblmüller, A. Terenzi, K. Holste, M. Haider, D. Baier, W. Berger, P. Heffeter, C. R. Kowol, B. K. Keppler, *ChemMedChem* **2016**, *11*, 2410.
- [26] R. M. Phillips, *Cancer Chemother. Pharmacol.* **2016**, *77*, 441.
- [27] W. R. Wilson, M. P. Hay, *Nat. Rev. Cancer* **2011**, *11*, 393.
- [28] L. F. Tietze, K. Schmuck, *Curr. Pharm. Des.* **2011**, *17*, 3527.
- [29] E. M. Williams, R. F. Little, A. M. Mowday, M. H. Rich, J. V. E. Chan-Hyams, J. N. Copp, J. B. Smail, A. V. Patterson, D. F. Ackerley, *Biochem. J.* **2015**, *471*, 131.
- [30] P. R. Race, A. L. Lovering, R. M. Green, A. Osson, S. A. White, P. F. Searle, C. J. Wrighton, E. I. Hyde, *J. Biol. Chem.* **2005**, *280*, 13256.
- [31] M. Lee, J. E. Simpson Jr., S. Woo, C. Kaenzig, G. M. Anlezark, E. Eno-Amooquaye, P. J. Burke, *Bioorg. Med. Chem. Lett.* **1997**, *7*, 1065.
- [32] M. P. Hay, G. J. Atwell, W. R. Wilson, S. M. Pullen, W. A. Denny, *J. Med. Chem.* **2003**, *46*, 2456.
- [33] A. Skwarska, E. D. D. Calder, D. Sneddon, H. Bolland, M. L. Odyniec, I. N. Mistry, J. Martin, L. K. Folkes, S. J. Conway, E. M. Hammond, *Cell Chem. Biol.* **2021**, *28*, 1258.
- [34] R. J. Knox, M. P. Boland, F. Friedlos, B. Coles, C. Southan, J. J. Roberts, *Biochem. Pharmacol.* **1988**, *37*, 4671.
- [35] T. D. Gruber, C. Krishnamurthy, J. B. Grimm, M. R. Tadross, L. M. Wysocki, Z. J. Gartner, L. D. Lavis, *ACS Chem. Biol.* **2018**, *13*, 2888.
- [36] E. D. D. Calder, A. Skwarska, D. Sneddon, L. K. Folkes, I. N. Mistry, S. J. Conway, E. M. Hammond, *Tetrahedron* **2020**, *76*, 131170.
- [37] E. M. Herrlinger, M. Hau, D. M. Redhaber, G. Greve, D. Willmann, S. Steimle, M. Müller, M. Lübbert, C. C. Miething, R. Schüle, M. Jung, *ChemBioChem* **2020**, *21*, 2329.
- [38] A. K. Ghosh, M. Brindisi, *J. Med. Chem.* **2015**, *58*, 2895.
- [39] A. Alouane, R. Labruère, T. Le Saux, F. Schmidt, L. Jullien, *Angew. Chem. Int. Ed.* **2015**, *54*, 7492.
- [40] M. Thomas, J. Clarhaut, I. Tranoy-Opalinski, J. P. Gesson, J. Roche, S. Papot, *Bioorg. Med. Chem.* **2008**, *16*, 8109.
- [41] M. Zessin, Z. Kutil, M. Meleshin, Z. Nováková, E. Ghazy, D. Kalbas, M. Marek, C. Romier, W. Sippl, C. Bařinka, M. Schutkowski, *Biochemistry* **2019**, *58*, 4777.
- [42] M. Abdelsalam, H. S. Ibrahim, L. Krauss, M. Zessin, A. Vecchio, S. Hastreiter, M. Schutkowski, G. Schneider, W. Sippl, *HDAC/HAT Function Assessment and Inhibitor Development: Methods and Protocols*, Springer US, New York, NY **2023**, p. 145.

SUPPORTING INFORMATION

Additional supporting information can be found online in the Supporting Information section at the end of this article.

How to cite this article: M. Abdelsalam, M. Zmysliá, K. Schmidtkunz, A. Vecchio, S. Hilscher, H. S. Ibrahim, M. Schutkowski, M. Jung, C. Jessen-Trefzer, W. Sippl, *Arch. Pharm.* **2024**;357:e2300536.
<https://doi.org/10.1002/ardp.202300536>